

RESEARCH PAPER

Fe-Ag Nanocomposite: Hydrothermal Preparation of Iron Nanoparticles and Silver Dendrite Like Nanostructures

Gholamreza Nabiyouni^{1*} and Davood Ghanbari²

¹ Department of Physics, Faculty of Science, Arak University, Arak, Iran

² Young Researchers and Elite Club, Arak Branch, Islamic Azad University, Arak, Iran

ARTICLE INFO

Article History:

Received 27 January 2017

Accepted 19 March 2017

Published 01 April 2017

Keywords:

Dendrite

Nanocomposite

Nanoparticles

Photo-catalyst

ABSTRACT

At the first stage Fe₃O₄ and Fe nanoparticles were synthesized via a simple hydrothermal method. Then silver nanoparticles and Fe-Ag nanocomposites were synthesized in the presence of NaBH₄. The prepared products were characterized by X-ray diffraction pattern, scanning electron microscopy, and Fourier transform infrared spectroscopy. Vibrating Sample magnetometer illustrated that Fe nanoparticles have super paramagnetic behaviour. The photo catalytic behaviour of Fe-Ag nanocomposites was investigated using the degradation of three various azo dyes under ultraviolet light irradiation. The results show that nanocomposites have feasible magnetic and photo catalytic properties.

How to cite this article

Nabiyouni Gh, Ghanbari D. Fe-Ag Nanocomposite: Hydrothermal Preparation of Iron Nanoparticles and Silver Dendrite Like Nanostructures. J Nanostruct, 2017; 7(2):111-120. DOI: 10.22052/jns.2017.02.004

INTRODUCTION

Interestingly hydrothermal is a specific procedure for synthesis of nanostructures with desired and controlled shape and dimensions. While predominant morphology in other methods like sol-gel, sonochemical is nanoparticle. Usually hydrothermal method leads to preferential growth in comparison to spherical nucleation. In hydrothermal method because of some particular conditions (high temperature and pressure) the nanoparticles grow in situ and form hierarchical structures [1-4]. Quantum confinement and large surface-to-volume ratio lead to distinct magnetic properties which are different from those of their bulk structures [1]. This behaviour has been explained as due to the large volume fractions of the atoms in the grain boundary area with unusual properties like spin canting, surface anisotropy, dislocations and super-paramagnetic behaviour. Magnetic separation is considered as a high speed and effective technique for separating magnetic particles. Thus, if the photocatalyst is

* Corresponding Author Email: G-Nabiyouni@araku.ac.ir

magnetic, it could be gathered conveniently by magnetic field [1,2]. Ferrites are technologically essential materials that are used in the fabrication of magnetic, electronic and microwave devices. These materials have a potential application at high frequency range due to their very low electrical conductivity, fairly large magneto-crystalline anisotropy, relatively large saturation magnetization, mechanical hardness and low production costs [3-4].

Hydrothermal synthesis can be defined as a method of synthesis of single crystals that depends on the solubility of minerals in hot water under high pressure. The crystal growth is performed in an apparatus consisting of a steel pressure vessel called an autoclave. A temperature gradient is maintained between the opposite ends of the growth chamber. At the hotter end the nutrient solute dissolves, while at the cooler end it is deposited on a seed crystal, growing the desired crystal. Also, materials which have a high vapour pressure near their melting points can

also be grown by the hydrothermal method. The method is also particularly suitable for the growth of large good-quality crystals while maintaining control over their composition. We have used hydrothermal method for this synthesis. There is a need to promote the experimental processes for the synthesis of nano-materials that offers ease in size control and stable preparation which could be used in wide range of applications. With the promotion of these new methods, the concern for environmental contamination is also heightened as chemical procedures generates a large amount of hazardous products [5-7]. Noble metals nanoparticles can strongly absorb visible light due to their localized surface plasmon resonance (LSPR), which can be adjusted by varying their size, surrounding and shape. When the frequency of the event light satisfies the resonance conditions of the noble-metal nanoparticles, the LSPR occurs with the associated light absorption. Moreover, noble metal nanoparticles can also work as an electron trap and active reaction sites [8-12]. Plasmon resonant nanostructures have gained remarkable interest in many fields, medicine, including near-field optics, surface enhanced spectroscopy, and solar cells. It was explored the applicability of plasmonic processes in the field of photocatalytic chemistry for organic molecule decomposition CO oxidation, and even materials synthesis. Various enhancement mechanisms have been proposed, comprising plasmonic heating and charge transfer [9, 10]. Noble metal nanoparticles have been the subject of extensive research in the frame of nanotechnology, mainly owing to their unique optical properties. Indeed, the free electron gas of such nanoparticles

features a resonant oscillation upon illumination in the visible part of the spectrum. The spectral properties of this resonance depend on the constitutive material, the shape of the nanoparticles and its environment. This resonant electronic oscillation is called localized surface plasmon (LSP), and the field of research that studies the fundamentals and applications of LSP is known as nanoplasmonics. LSPs are accompanied by valuable physical effects such as optical near-field enhancement, heat generation and excitation of hot-electrons. Hence, plasmonic nanoparticles can behave as efficient nanosources of heat, light or energetic electrons, remotely controllable by light [11,12]. The composites of semiconductor nanoparticles and optically active metallic nanostructures represent a promising alternative to conventional photocatalysts. The main feature of these photocatalysts is that the interaction between semiconductor and metallic building blocks results in very efficient conversion of incident photons into electron-hole pairs in the semiconductor [12-15].

In this work Fe-Ag nanocomposites were synthesized by hydrothermal method. The photocatalytic behaviour of Fe-Ag nanocomposites was evaluated using the degradation of three various azo dyes under ultraviolet light irradiation. The results show that nanocomposites have applicable super paramagnetic and photocatalytic performance.

MATERIALS AND METHODS

$\text{FeCl}_2 \cdot 4\text{H}_2\text{O}$, AgNO_3 , NaBH_4 , ammonia and distilled water were purchased from Merck Company was prepared. Scanning electron

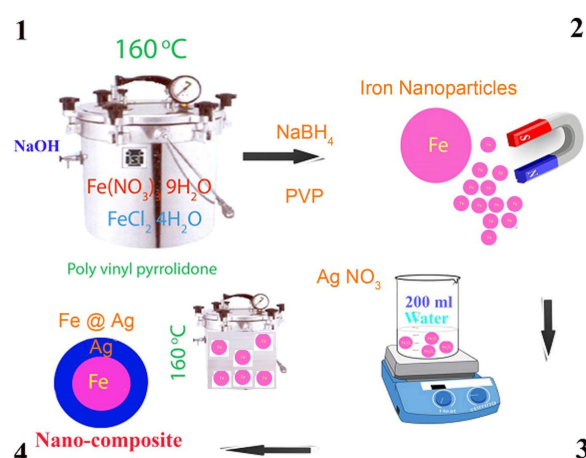


Fig. 1. Schematic of nanocomposite preparation

microscopy images were obtained using a LEO instrument model 1455VP. All the chemicals were used as received without further purifications. Before to taking images, the samples were coated by a very thin layer of Pt (using a BAL-TEC SCD 005 sputter coater) to make the sample surface conductor and prevent charge accumulation, and obtaining a better contrast. A multiwave ultrasonic generator (Bandeline MS 73), equipped with a converter/transducer and titanium oscillator, operating at 20 kHz with a maximum power output of 150 W was used for the ultrasonic irradiation. X-ray diffraction patterns were recorded by a Philips, X-ray diffractometer using Ni-filtered $\text{CuK}\alpha$ radiation. Room temperature magnetic properties were investigated using a vibrating sample magnetometer (VSM) device, (Meghnatis Kavir Kashan Co., Iran) in an applied magnetic field sweeping between ± 10000 Oe.

Preparation of Fe nanoparticles

0.001 mol of $\text{FeCl}_2 \cdot 4\text{H}_2\text{O}$ was dissolved in 200 mL of distilled water. Then 1 ml of NaBH_4 as surfactant was added to the solution, it was mixed on magnetic stirring for 10 min. 16ml of NH_3 (1M) as precipitator was slowly added to reaching pH of solution to 10. The solution is put into an autoclave and oven at 160°C for 5 hours. The obtained black precipitate was washed twice with distilled water. Then it was dried in oven for 24h .

Preparation of Fe-Ag nanocomposites

Firstly 0.1 g of synthesized iron nanoparticles was dispersed in 200 ml of distilled water and then 0.2g of AgNO_3 was then dissolved in the solution.

Then 1 ml of NaBH_4 as reducing agent was added to the solution and was mixed for 2h. The solution is put into an autoclave and oven at 160°C for 5 hours. (Fig.1).

Photo-catalyst investigation

10 ml of the dye solution (20 ppm) was used as a model pollutant to determine the photocatalytic activity. 0.1 g of catalyst was applied for degradation of 10 ml solution. The solution was mixed by a magnet stirrer for 1 hour in darkness to determine the adsorption of the dye by catalyst and better availability of the surface. The solution was irradiated by a 10 W UV lamp which was placed in a quartz pipe in the middle of reactor. It was turned on after 1 hour stirring the solution and sampling (about 10 ml) was done every 15 min. The samples were filtered, centrifuged and their concentration was determined by UV-Visible spectrometry.

RESULTS AND DISCUSSION

Fig. 2 illustrates XRD pattern of product without using capping agent and by using low amount of NaBH_4 . It can be observed that cubic phase (JCPDS No.74-0748) with Fd-3m space group which is consistent with pure magnetite was prepared. Fig. 3 shows XRD pattern of pure iron product (JCPDS No 06-0696). Fig. 4 shows XRD pattern of silver product. A number of strong Bragg reflection peaks can be seen which correspond to the (111), (200), (220) and (311) reflections of FCC silver and lattice parameters of $a = b = c = 4.070 \text{ \AA}$. The standards (JCPDS), silver file No. 04-0783 and space group of Fm-3m (space group number: 225) in the pattern

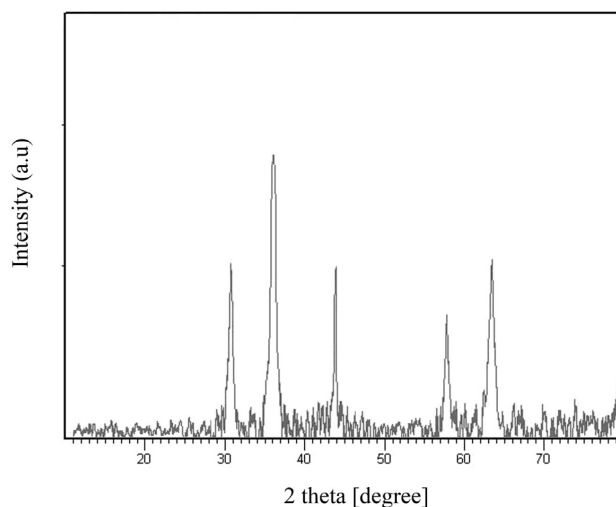


Fig. 2. XRD pattern of Fe_3O_4 nanoparticles

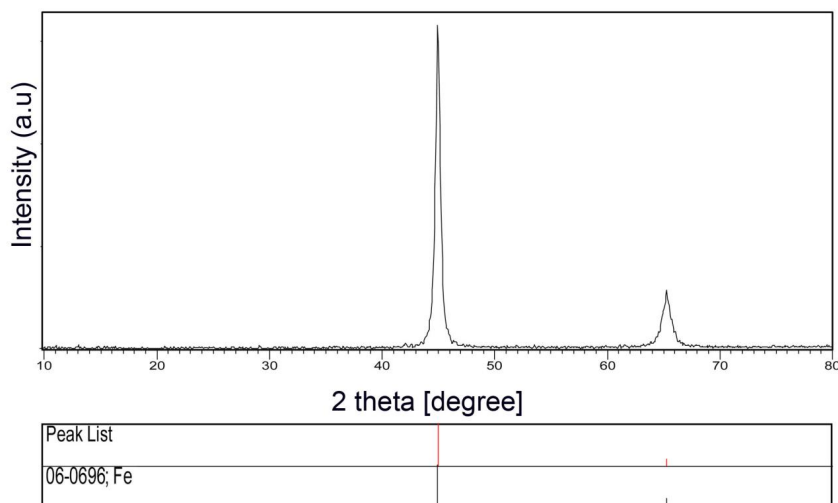


Fig. 3. XRD pattern of Fe nanoparticles

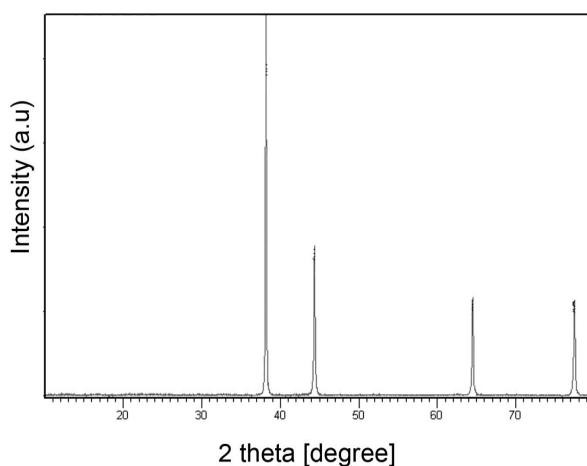


Fig. 4. XRD pattern of Ag nanoparticles

are reported. The calculated crystalline sizes from Scherrer equation, $D_c = K\lambda / \beta \cos\theta$, where β is the width of the observed diffraction peak at its half maximum intensity (FWHM), K is the shape factor, which takes a value of about 0.9, and λ is the X-ray wavelength (CuK_α radiation, equals to 0.154 nm) were about 22 and 32 nm for Fe and Ag nanoparticles, respectively

By using not efficient NaBH_4 magnetite was synthesized. SEM images of the as-synthesized Fe_3O_4 nanoparticles are illustrated in Fig. 5. Nucleation stage overcomes to growth stage the and nanoparticles with average particle size less than 40 nm were synthesized.

Concentration effect of reducing agent and capping agent (PVP) was also examined. SEM images of the synthesized Fe nanoparticles with 10 ml of NaBH_4 as capping agent are shown in Fig.

6. Results confirm by enhancement of NaBH_4 , pure iron with average diameter size less than 90 nm were prepared.

The effect of temperature was also tested; Fig. 7 depict SEM images of the synthesized Fe nanoparticles with 10 ml of NaBH_4 as reducing agent by hydrothermal method and heated in autoclave at 200 °C for 5h. Images approve nanoparticles with average diameter size less than 50 nm were prepared.

SEM images of the synthesized Ag nanoparticles with 1ml of NaBH_4 as reducing agent by hydrothermal method and heated in autoclave at 160 °C in 5 h are shown in Fig. 8. Images confirm dendrite like nanoparticles with average diameter size less than 20 nm were prepared.

Reaction time was investigated, Fig. 9 illustrate SEM images of the synthesized Ag nanoparticles

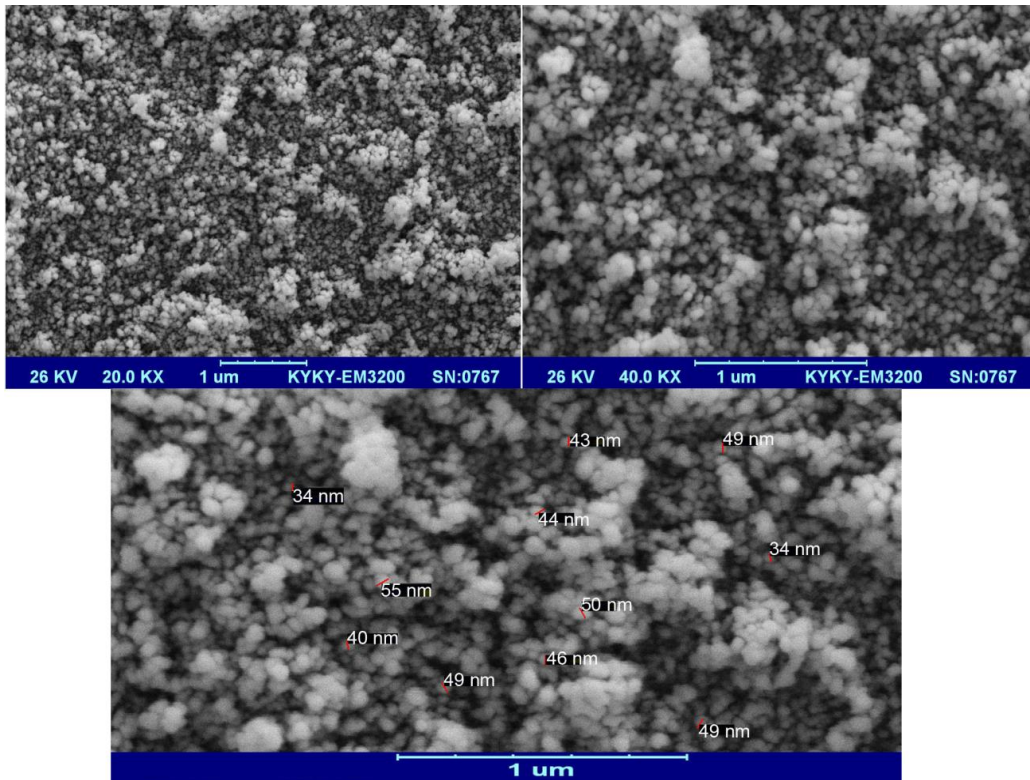


Fig. 5. SEM images of Fe_3O_4

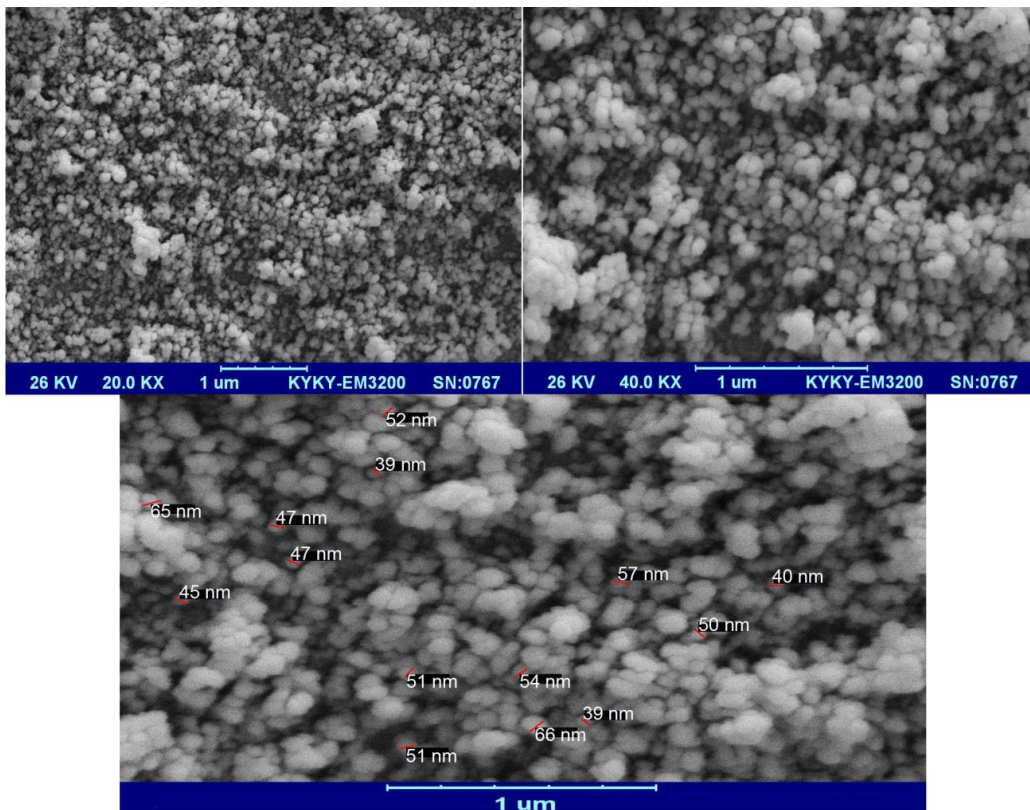


Fig. 6. SEM images of Fe with PVP

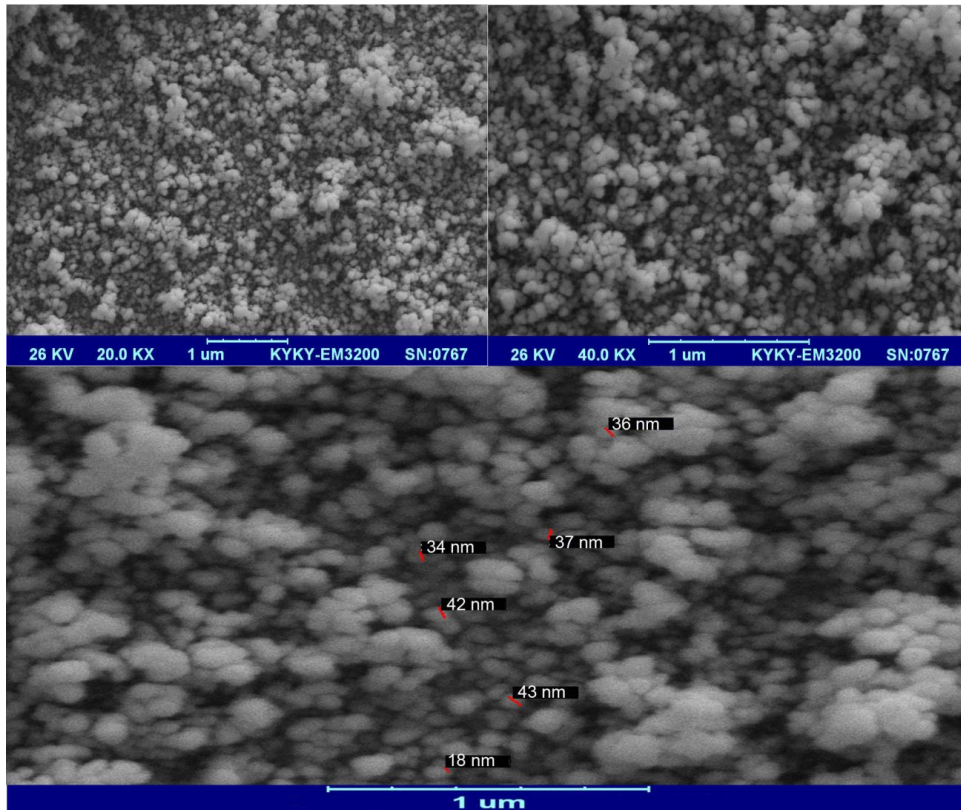


Fig. 7. SEM images of Fe prepared at 200 °C

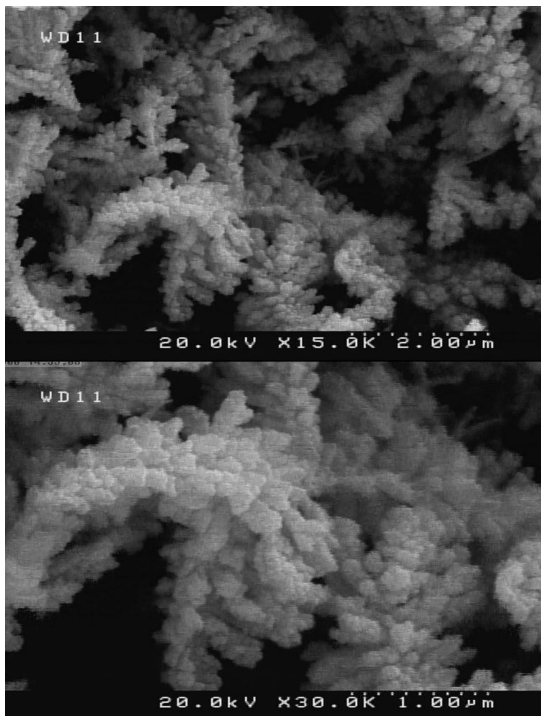


Fig. 8. SEM images of Ag prepared at 160 °C for 5h



Fig. 9. SEM images of Ag synthesized at 160 °C for 10 h

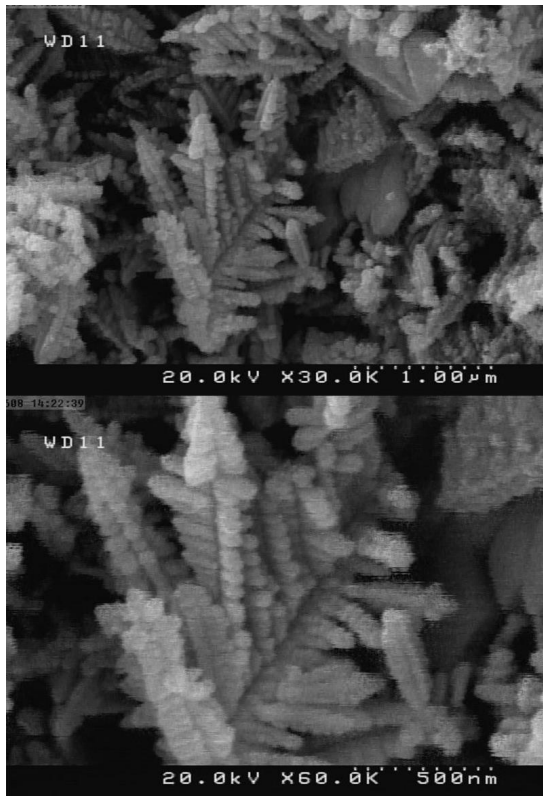


Fig. 10. SEM images of nanocomposite prepared at 160 °C for 5h

with 1 ml of NaBH_4 at 160 °C for 10h. Results confirm flower like nanostructures were prepared and nanoparticles with average diameter size less than 90 nm were obtained.

It is known that the particle size and morphology can be manipulated by adjusting the super-

saturation during the nucleation and crystal growth in hydrothermal, which in turn, it can strongly be affected by solution chemistry of hydrothermal conditions such as reaction temperature depends on precursor, time and temperature and pH of process environment.

Fig. 10 show SEM images of nanocomposites at 160 °C for 5h. Images approve formation of dendrite like nanostructures with average particle size around 50 nm. The balance between nucleation rate and growth rate which determines final particle size and morphology

Magnetic properties of samples were studied using vibrating sample magnetometer system at room temperature. Hysteresis loop of magnetic Fe_3O_4 nanoparticles at 160°C is shown in Fig. 11. Nanoparticles show super paramagnetic behaviour and have a saturation magnetization of 58 emu/g and a coercivity tending to zero Oe. It shows a sufficient magnetization of these nanoparticles for being recycled by a magnet, making them appropriate for core of recyclable photo-catalyst.

As-synthesized Fe nanoparticles show super paramagnetic behaviour and have a saturation magnetization of 87 emu/g and a coercivity tending to 10 Oe (Fig. 12).

Hysteresis loop of magnetic Fe-Ag 10% nanoparticles prepared by simple hydrothermal is depicted in Fig. 13. The product also illustrates super paramagnetic behaviour and has a saturation magnetization of 75 emu/g and a coercivity about zero Oe.

Fig. 14 shows hysteresis loop of magnetic Fe₃Ag

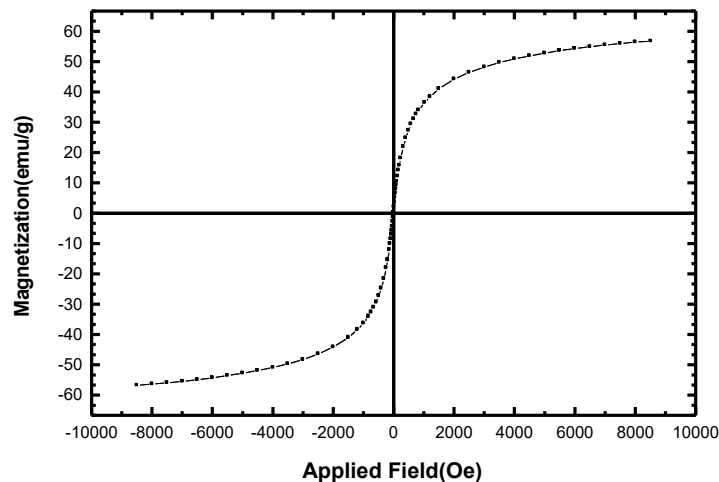


Fig. 11. Room temperature hysteresis loop of Fe_3O_4 nanoparticles

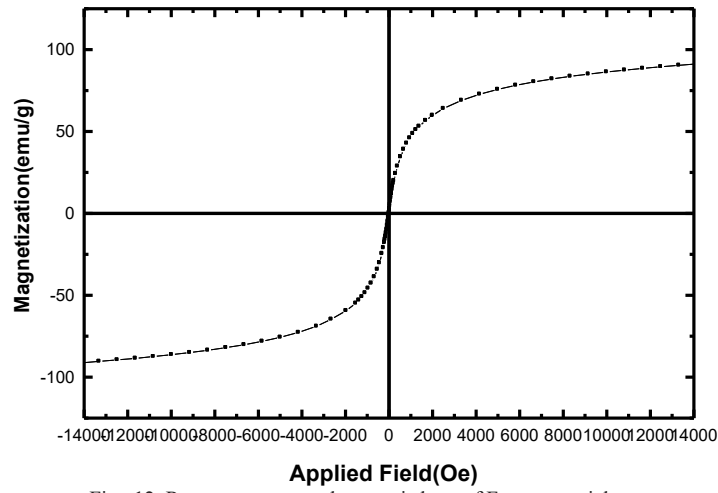


Fig. 12. Room temperature hysteresis loop of Fe nanoparticles

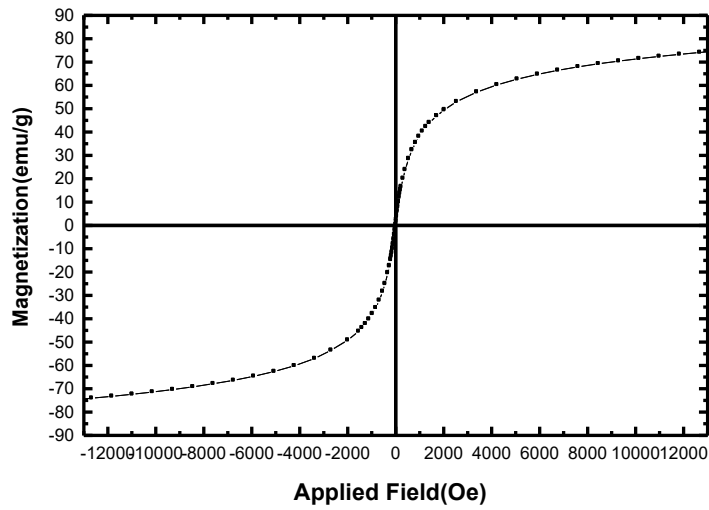


Fig. 13. VSM curve of Fe-Ag 10% nanocomposites

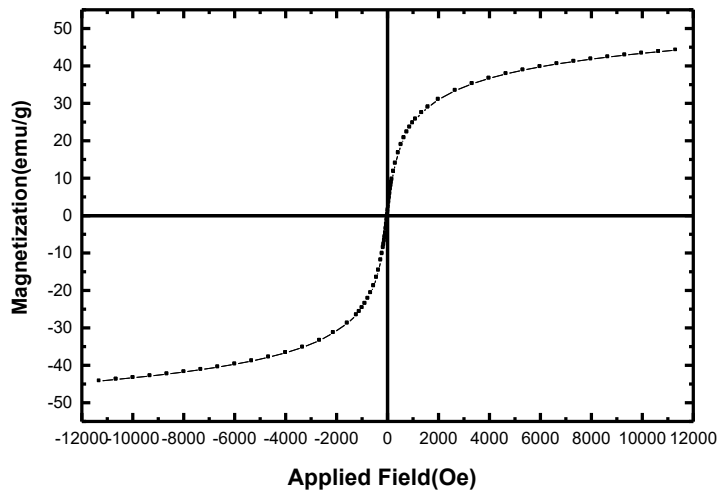


Fig. 14. Hysteresis curve of Fe- Ag 50%:50% nanocomposite

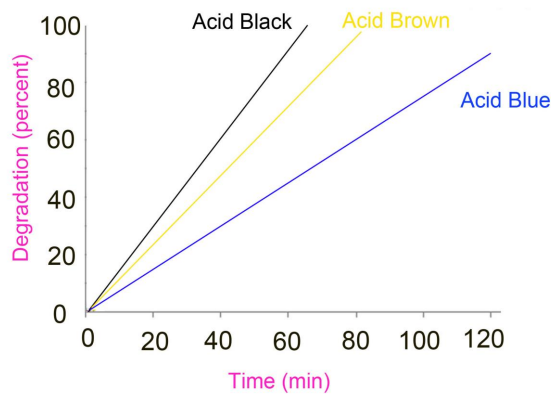


Fig. 15. Photo degradation of (a) Acid Brown (b) Acid Black (c) Acid Blue

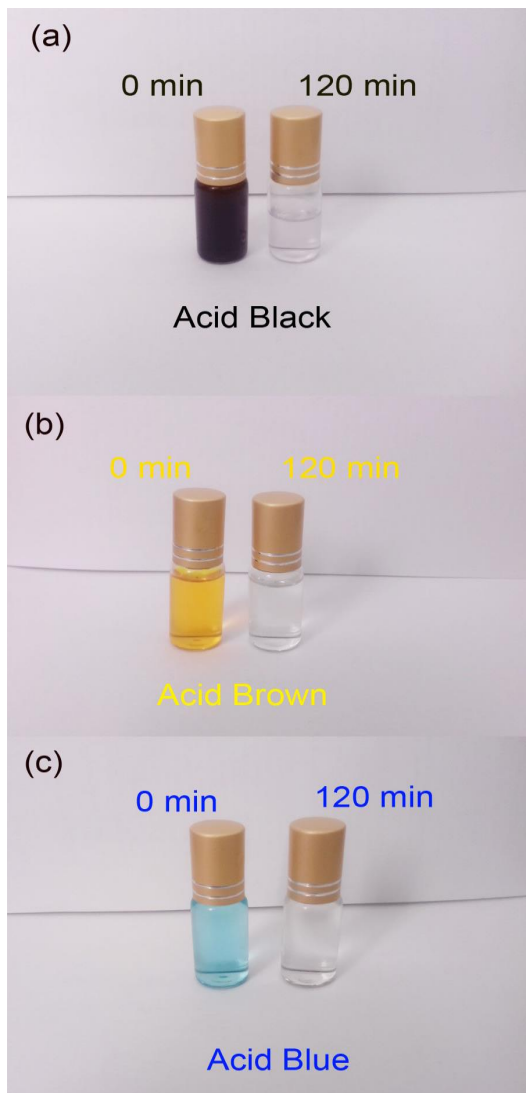


Fig. 16. Photo degradation of (a) Acid Black (b) Acid Brown (c) Acid Blue

50% nanoparticles prepared by hydrothermal at 180 °C. Nano-spheres show super paramagnetic behaviour and have a saturation magnetization of 44 emu/g and a coercivity about zero Oe. This magnetization indicates that Fe-Ag nanocomposites inherit the magnetic property from the Fe; however, the magnetization is lower due to presence of silver. This reduction in saturation magnetization is due to the interfacial effect of the typical nanocomposite. The magnetic property of the prepared nanocomposites is an essential characteristic of a re-generable and reusable magnetic heterogeneous catalyst.

The photo-catalytic activity of the Fe-Ag nanocomposite was evaluated by monitoring the degradation of Acid-Brown , Acid Blue, Acid Black in an aqueous solution, under irradiation with UV light. The changes in the intensity of maximum wave length of four azo-dyes are depicted in Fig. 15. Maximum wave length of Acid Black, Acid-Brown and Acid Blue were degraded about 98%, 97% and 85% in 120 min in the presence of magnetite-silver. Acid brown showed the fastest degradation at 40 min under ultraviolet light and at presence of magnetic photo-catalyst. Organic dyes decompose to carbon dioxide, water and other less toxic or nontoxic residuals [11-17]. Fig. 16 shows degradation of the three azo dyes after 120 min exposure to the Fe-Ag nanocomposite.

CONCLUSIONS

Firstly magnetite nanoparticles were synthesized via a hydrothermal in the presence of NaBH_4 , then silver nanoparticles and Fe-Ag nanocomposites were prepared by hydrothermal method. Effect of temperature, reaction time and various concentration of NaBH_4 were investigated on the morphology and particle size of the products. Vibrating sample magnetometer confirmed that nanocomposites exhibit super-paramagnetic behaviour. The photocatalytic behaviour of Fe-Ag nanocomposite was evaluated using the degradation of three azo dyes under UV-visible light irradiation. The results show that hydrothermal method is suitable method for preparation of Fe-Ag nanocomposites as a candidate for photocatalytic applications.

ACKNOWLEDGEMENTS

This work has been supported financially by Arak University Research Council (AURC) under the Grant Number of 94-9329.

CONFLICT OF INTEREST

The authors declare that there are no conflicts of interest regarding the publication of this manuscript.

REFERENCES

1. Asiabani N, Nabiyouni G, Khaghani S, Ghanbari D, Green synthesis of magnetic and photo-catalyst PbFe₁₂O₁₉-PbS nanocomposites by lemon extract: nano-sphere PbFe₁₂O₁₉ and star-like PbS. *J. Mater. Sci. Mater. Electron*, 2017;28: 1101-1114
2. Khaghani S, Ghanbari D, Magnetic and photo-catalyst Fe₃O₄-Ag nanocomposite: green preparation of silver and magnetite nanoparticles by garlic extract. *J. Mater. Sci. Mater. Electron*, 2017; 28 2877-2886:
3. Jacobo S E, Civale L, Blesa M A. Evolution of the magnetic properties during the thermal treatment of barium hexaferrite precursors obtained by coprecipitation from barium ferrate (VI) solutions. *J Magnet Magnet Mater*. 2000; 260: 37-41.
4. Dorsey P C, Qadri S B, Grabowski K S, Knies D L, Lubitz P, Chrisley D B, Hortwitz J S, Epitaxial Pb-Fe-O film with large planar magnetic anisotropy on (0001) sapphire. *Appl Phys Lett*. 1997;70: 1173-1175.
5. Nabiyouni G; Ghanbari D; Ghasemi J; Yousofnejad A, Microwave-assisted Synthesis of MgFe₂O₄-ZnO Nanocomposite and Its Photo-catalyst Investigation in Methyl Orange Degradation. *J Nanostruct*. 2015; 5 (3): 289-295.
6. Jalajjerdi R, Ghanbari D, Microwave Synthesis and Magnetic Investigation of CuFe₂O₄ Nanoparticles and Poly Styrene-Carbon Nanotubes Composites. *J Nanostruct*. 2016; 6 (4): 278-284.
7. Jalajjerdi R, F. Gholamian F, Shafie H, Moraveji A, Ghanbari D, Thermal and Magnetic Characteristics of Cellulose Acetate-Fe₃O₄. *J Nanostruct*. 2011; 1 (2): 105-109.
8. Tokar M. Microstructure and Magnetic Properties of Lead Ferrite. *J Amer Ceram Soc*. 1969; 52: 302-306.
9. Horikoshi S, Serpone N. *Microwaves in nanoparticle synthesis: fundamentals and applications*. John Wiley & Sons. 2013.
10. Shinohara N. Power without wires. *IEEE Microwave Magazine*, 2011; 12: S64-S73.
11. Tompsett G A, Conner W.C, Yngvesson K S. Microwave synthesis of nanoporous materials. *ChemPhysChem*, 2006; 7: 296-319.
12. Nabiyouni G, Ghanbari D, A. Yousofnejad A, Seraj M, Mirdamadian Z, Microwave-Assisted Synthesis of CuFe₂O₄ Nanoparticles and Starch-Based Magnetic Nanocomposites. *J Nanostruct*. 2013; 3 (2): 155-160.
13. Ghanbari D, Salavati-Niasari M. Synthesis of urchin-like CdS-Fe₃O₄ nanocomposite and its application in flame retardancy of magnetic cellulose acetate. *J Ind Eng Chem*. 2015; 24: 284-292.
14. Nabiyouni G, Sharifi S, Ghanbari D, Salavati-Niasari M, A Simple Precipitation Method for Synthesis CoFe₂O₄ Nanoparticles. *J Nanostruct*. 2014; 4(3): 317-323.
15. Ghanbari D, Salavati-Niasari M. Hydrothermal synthesis of different morphologies of MgFe₂O₄ and magnetic cellulose acetate nanocomposite. *Kor J Chem Eng*. 2015; 32(5): 903-910
16. Ghanbari D, Salavati-Niasari M, Ghasemi-Kooch M. In situ and ex situ synthesis of poly (vinyl alcohol)-Fe₃O₄ nanocomposite flame retardants. *Particuology*, 2016; 26: 87-94.
17. Ghanbari D, Sharifi S, Naraghi A, Nabiyouni G, Photo-degradation of azo-dyes by applicable magnetic zeolite Y-Silver-CoFe₂O₄ nanocomposites, *J. Mater. Sci. Mater. Electron* , 2016; 27: 5315-5323